THE JOURNAL OF BIOLOGICAL CHEMISTRY
Vol. 274, No. 22, Issue of May 28, pp. 15775–15780, 1999

Printed in U.S.A.

Absence of Spontaneous Peroxisome Proliferation in Enoyl-CoA Hydratase/L-3-Hydroxyacyl-CoA Dehydrogenase-deficient Mouse Liver

FURTHER SUPPORT FOR THE ROLE OF FATTY ACYL CoA OXIDASE IN PPARα LIGAND METABOLISM*

(Received for publication, February 19, 1999, and in revised form, March 15, 1999)

Chao Qi‡, Yijun Zhu‡, Jie Pan‡, Nobuteru Usuda‡, Nobuyo Maeda§, Anjana V. Yeldandi‡, M. Sambasiva Rao‡, Takashi Hashimoto‡, and Janardan K. Reddy‡¶

From the ‡Department of Pathology, Northwestern University Medical School, Chicago, Illinois 60611-3008 and the §Department of Pathology, University of North Carolina, Chapel Hill, North Carolina, 27599

Peroxisomes contain a classical L-hydroxy-specific peroxisome proliferator-inducible β-oxidation system and also a second noninducible D-hydroxy-specific β-oxidation system. We previously generated mice lacking fatty acyl-CoA oxidase (AOX), the first enzyme of the L-hydroxy-specific classical β-oxidation system; these AOX$^{-/-}$ mice exhibited sustained activation of peroxisome proliferator-activated receptor α (PPARα), resulting in profound spontaneous peroxisome proliferation in liver cells. These observations implied that AOX is responsible for the metabolic degradation of PPARα ligands. In this study, the function of enoyl-CoA hydratase/L-3-hydroxyacyl-CoA dehydrogenase (L-PBE), the second enzyme of this peroxisomal β-oxidation system, was investigated by disrupting its gene. Mutant mice (L-PBE$^{-/-}$) were viable and fertile and exhibited no detectable gross phenotypic defects. L-PBE$^{-/-}$ mice showed no hepatic steatosis and manifested no spontaneous peroxisome proliferation, unlike that encountered in livers of mice deficient in AOX. These results indicate that disruption of classical peroxisomal fatty acid β-oxidation system distal to AOX step does not interfere with the inactivation of endogenous ligands of PPARα, further confirming that the AOX gene is indispensable for the physiological regulation of this receptor. The absence of appreciable changes in lipid metabolism also indicates that enoyl-CoAs, generated in the classical system in L-PBE$^{-/-}$ mice are diverted to D-hydroxy-specific system for metabolism by D-PBE. When challenged with a peroxisome proliferator, L-PBE$^{-/-}$ mice showed increases in the levels of hepatic mRNAs and proteins that are regulated by PPARα except for appreciable blunting of peroxisome proliferative response as compared with that observed in hepatocytes of wild type mice similarly treated. This blunting of peroxisome proliferative response is attributed to the absence of L-PBE protein in L-PBE$^{-/-}$ mouse liver, because all other proteins are induced essentially to the same extent in both wild type and L-PBE$^{-/-}$ mice.

In animal cells, mitochondria, as well as peroxisomes, oxidize fatty acids via β-oxidation, with long chain and very long chain fatty acids being preferentially oxidized by peroxisomes (1–3). Peroxisomal β-oxidation process is carried out by two distinct groups of enzymes; the classical first group utilizes straight chain saturated fatty acyl-CoAs as substrates, whereas the recently discovered second group acts on branched chain acyl-CoAs (3, 4). In the L-hydroxy-specific classical β-oxidation spiral, dehydrogenation of acyl-CoA esters to their corresponding *trans*-2-enoyl-CoAs is catalyzed by fatty acyl-CoA oxidase (AOX),[1] whereas the second and third reactions, hydration and dehydrogenation of enoyl-CoA esters to 3-ketoacyl-CoA, are carried out by a single enzyme, enoyl-CoA hydratase/L-3-hydroxyacyl-CoA dehydrogenase (L-bifunctional enzyme (L-PBE)) (3). The third enzyme of this classical system, 3-ketoacyl-CoA thiolase (PTL) cleaves 3-ketoacyl-CoAs to acetyl-CoA, and an acyl-CoA that is two carbon atoms shorter than the original molecule can re-enter the β-oxidation spiral (1, 2). In the second D-hydroxy-specific β-oxidation pathway, dehydrogenation of acyl-CoA esters to their corresponding *trans*-2-enoyl-CoAs is catalyzed by the branched chain acyl-CoA oxidase (2), with the recently identified D-3-hydroxyacyl-CoA dehydratase/D-3-hydroxyacl-CoA dehydrogenase (D-bifunctional enzyme (D-PBE)), converting enoyl-CoAs to 3-ketoacyl-CoAs via D-3-hydroxyacyl-CoAs (3, 4). The third enzyme of this second system is designated as sterol carrier protein x (SCPx), which possesses 3-ketoacyl-CoA thiolase activity (5).

Of these two peroxisomal β-oxidation systems, the enzymes belonging to the classical group are markedly induced in the liver of rats and mice in conjunction with profound proliferation of peroxisomes by a group of structurally diverse agents designated as peroxisome proliferators (6). They exert their pleiotropic effects by activating a nuclear receptor called peroxisome proliferator-activated receptor α (PPARα) (7). Sustained induction of PPARα-mediated peroxisome proliferation and transcriptional activation of classical β-oxidation system genes lead to the development of liver tumors in rats and mice (8). It is postulated that H_2O_2 overproduced by the induction of

* This work was supported by National Institutes of Health Grant GM 23750 (to J. K. R.), Veterans Affairs merit review grants (to A. V. Y. and M. S. R.), and Joseph L. Mayberry, Sr. Endowment Fund. The costs of publication of this article were defrayed in part by the payment of page charges. This article must therefore be hereby marked "*advertisement*" in accordance with 18 U.S.C. Section 1734 solely to indicate this fact.

¶ To whom correspondence should be addressed: Dept. of Pathology, Northwestern University Medical School, 303 East Chicago Ave., Chicago, IL 60611-3008. Tel.: 312-503-7948; Fax: 312-503-8249; E-mail: jkreddy@nwu.edu.

[1] The abbreviations used are: AOX, straight chain fatty acyl-CoA oxidase or palmitoyl-CoA oxidase; PPAR, peroxisome proliferator-activated receptor; L-PBE, enoyl-CoA hydratase/L-3-hydroxyacyl-CoA dehydrogenase (L-bifunctional enzyme); D-PBE, D-3-hydroxyacyl-CoA dehydratase/D-3-hydroxyacyl CoA-dehydrogenase (D-bifunctional enzyme); PTL, peroxisomal 3-ketoacyl-CoA thiolase; CYP4A1 and CYP4A3, encode microsomal cytochrome P450 fatty acid ω-hydroxylases; SCPx, sterol carrier protein x or 3-ketoacyl-CoA thiolase/sterol carrier protein 2; LCAD, long-chain acyl-CoA dehydrogenase; VLCAD, very LCAD; CTL, catalase; ES, embryonic stem cells; kb, kilobase(s).

this β-oxidation system and cell proliferation contribute to hepatocarcinogenesis in livers with peroxisome proliferation (8, 9). To investigate the functional implications of PPARα-regulated L-hydroxy-specific β-oxidation system, we recently generated mice deficient in AOX, the first enzyme of this inducible system, and found that they exhibit steatohepatitis and spontaneous peroxisome proliferation in liver cells (10). These results suggested that straight chain acyl-CoAs and other putative substrates for classical AOX serve as natural ligands for PPARα, and this enzyme is indispensable for the physiological regulation of PPARα (10). Here, we describe the generation of mice homozygous for a disruption of the L-PBE gene, which encodes the second enzyme of this β-oxidation spiral and report that these mice do not exhibit phenotypic alterations such as those found in AOX null mice, further confirming that disruption of this classical β-oxidation pathway distal to AOX does not affect the metabolism of natural ligands of PPARα.

MATERIALS AND METHODS

Gene Targeting—P1 genomic clone (6346) containing the L-PBE gene was obtained by screening a mouse 129/Sv P1 bacteriophage library (Genome Systems, St. Louis, MO) using polymerase chain reaction with primers 5′-GTGCTGATATCCATGGCTTTAGTG-3′and 5′-GATAGTGACAGCCCAAGGCCAGCTC-3′ (11). The targeting construct was assembled in the pPNT targeting vector with the 2.5-kb *Xba*I fragment from the *Sac*I subclone and 4-kb *Xba*I/*Apa*I fragment from the *Apa*I subclone serving as the 5′ and 3′ homologous regions, respectively, of the phosphoglycerate kinase promoter/neomycin-resistance gene (Neo) (Fig. 1*A*). The targeting vector also contained the herpes simplex thymidine kinase (*hsv-tk*) gene, which allowed the use of a positive-negative selection scheme. The final construct, designated pPNT-L-PBE, is illustrated in Fig. 1*A*.

Generation of L-PBE Mutant Mice—*Not*I-linearized targeting vector (30 μg) was electroporated into BK4 embryonic stem (ES) cells and selected in 200 μg/ml G418 and 2 μM ganciclovir, and resistant colonies were subjected to Southern analysis. Two positive ES clones were injected into 3.5-day-old C57BL/6J blastocysts and transferred into pseudopregnant CBAF1 foster female recipients. The resulting chimeras were mated with C57BL/6J mice, and germ-line transmission was ascertained by coat color and confirmed by Southern analysis of genomic DNA (5 μg) isolated from tails, transferred to nitrocellulose membrane, and hybridized with probe 1 and probe 2 (Fig. 1*A*) at 42 °C in hybridization solution containing 50% formamide (12). F1 heterozygous siblings for the disrupted PBE gene were then mated to obtain homozygous PBE null mice.

Genotype of L-PBE Mutant Mice—The offspring from subsequent breeding were genotyped by polymerase chain reaction amplification and confirmed by Southern analysis as needed. Two primers, primers P1 (5′-GAGCTGGCCTTGGGCTGTCACTA-3′) and P2 (5′-TAGAAGCTGCGTTCCTCTTGCACCA-3′), derived from exons 3 and 4 of L-PBE gene, respectively, shown in Fig. 1*A* were designed to detect wild type allele, and two primers, primers P3 (5′-TGAATGAACTGCAGGACGAGG-3′) and P4 (5′-CCACAGTCGATGAATCCAGAA-3′), from the neomycin cassette were used to detect the PBE gene-targeted allele.

Treatment with Peroxisome Proliferators and Morphological Studies—Mice were fed powdered diet with or without a PPARα ligand, ciprofibrate (0.0125% w/w), or Wy-14,643 (0.1% w/w) for 4 to 14 days. For light microscopy, tissues were fixed in 10% neutral-buffered formalin and embedded in paraffin using standard procedures. Sections (4-μm thick) were cut and stained with hematoxylin and eosin. For cytochemical localization of catalase (CTL), tissues were processed and examined as described elsewhere (10). Immunocytochemical localization of CTL and L-PBE was performed using protein A-gold technique as described elsewhere (13). To assess liver cell proliferation, some mice were given bromodeoxyuridine (0.5 mg/ml) in drinking water for 3 days, and their livers were processed for immunohistochemistry. $AOX^{-/-}$ mice utilized in these studies were as described (10).

Western Blot Analysis and Fatty Acid Oxidation—Contents of β-oxidation enzymes and other proteins in liver were determined by immunoblot analysis using rabbit polyclonal antibodies against rat acyl-CoA synthetase, AOX, L-PBE, D-PBE, PTL, carnitine octanoyltransferase, urate oxidase, short chain acyl-CoA dehydrogenase, medium chain acyl-CoA dehydrogenase, very long chain and long chain acyl-CoA dehydrogenases (VLCAD and LCAD, respectively), SCPx, and CTL, as described (14). Fatty acid β-oxidation activity was measured using radioactive fatty acids (ICN Pharmaceuticals) and postnuclear fractions from livers as described (14).

Northern Hybridization—Total RNA (20 μg) extracted from the liver of wild type, L-$PBE^{-/-}$, and $AOX^{-/-}$ mice by Trizol reagent (Life Technologies, Inc.), was glyoxylated, separated on 0.8% agarose gel, and transferred to nylon membrane. Hybridization was performed at 42 °C in 50% formamide hybridization solution (12) using cDNA probes acyl-CoA synthetase, AOX, L-PBE, D-PBE, PTL, cytochrome P450 ω-hydroxylases (CYP4A1, CYP4A3), fatty acid-binding protein, and ribosomal RNA (28 S) as described (10). Changes in mRNA levels were estimated by densitometric scanning of autoradiograms.

RESULTS

Generation of L-$PBE^{-/-}$ Mice—The targeting construct illustrated in Fig. 1 was used to disrupt the L-PBE gene in ES cells. Screening of 100 G418 ganciclovir-resistant colonies by Southern blotting yielded 5 homologous recombinants for a targeting frequency of 5%. ES cells from two different colonies were injected into C57BL/6J blastocysts to generate chimeric animals. Chimeras from both lines were able to transmit the mutant allele to their offspring after outbreeding with C57BL/6J. Genomic DNA from wild type mice when digested with *Bam*HI and *Eco*RI and probed with probe 1 yielded a single 4.3-kb fragment, and in L-$PBE^{+/-}$ mouse DNA, two bands, 6.1 and 4.3 kb, were visualized (Fig. 1*B*). In L-$PBE^{-/-}$ mice, there is a single 6.1-kb band, indicating that both alleles were modified (Fig. 1*B*). At 2 weeks of age, the F1 progeny exhibited a predicted frequency of 25% homozygous mutant offspring (L-$PBE^{-/-}$), indicating no lethality associated with the null allele. L-$PBE^{-/-}$ mice exhibited no growth retardation during the first 4 weeks and displayed no apparent morphological abnormalities. Both male and female homozygous mice were fertile. Northern blot analysis using poly$(A)^+$ RNA isolated from liver showed an absence of L-PBE mRNA in L-$PBE^{-/-}$ mouse (Fig. 1*C*). Western blotting performed with anti-L-PBE antibody revealed the presence of two bands close to each other in wild type mouse liver (Fig. 1*D*). One of these proteins (the *lower band*) was confirmed to be L-PBE, because it disappeared when the antibodies were preincubated with purified rat L-PBE protein. The upper nonspecific band cross-reacting with anti-PBE antibody is present in mitochondrial and not in peroxisomal fraction (data not shown). In L-$PBE^{-/-}$mouse liver, we also detected this cross-reacting protein (*upper band*) but found no authentic L-PBE protein. Immunohistochemically, L-PBE staining appeared highly prominent in the liver of a wild type mouse treated with a peroxisome proliferator for 2 weeks, whereas no staining was evident in L-$PBE^{-/-}$ mouse liver (Fig. 2). The absence of L-PBE protein in L-$PBE^{-/-}$ mouse liver peroxisomes was further confirmed at the ultrastructural level by protein A-gold immunocytochemical procedure (Fig. 3).

Characterization of Liver Phenotype in L-$PBE^{-/-}$ Mice and Comparison with Mice Deficient in AOX—The histological architecture of liver as well as the appearance of hepatocytes in L-$PBE^{-/-}$ mice did not differ significantly from that of wild type animals (Fig. 4*A* and *B*). Of particular interest is that mice deficient in L-PBE displayed no hepatic fatty metamorphosis, a feature that is striking in young AOX deficient mice (Fig. 4*C*). Progressive hepatocellular regeneration occurring in older $AOX^{-/-}$mice leads to the emergence of hepatocytes with abundant eosinophilic cytoplasm suggestive of spontaneous peroxisome proliferation (Fig. 4, *C* and *D*). We then surveyed for alterations, if any, in peroxisome population in liver cells of L-$PBE^{-/-}$ mice to ascertain if deficiency of this enzyme also leads to spontaneous peroxisome proliferation such as that encountered in $AOX^{-/-}$ mice (10). Peroxisomes can be visualized at the light microscopic level in sections processed cytochemically for localizing peroxisomal marker enzyme catalase (10). In L-$PBE^{-/-}$ mouse hepatocytes, peroxisomes are few,

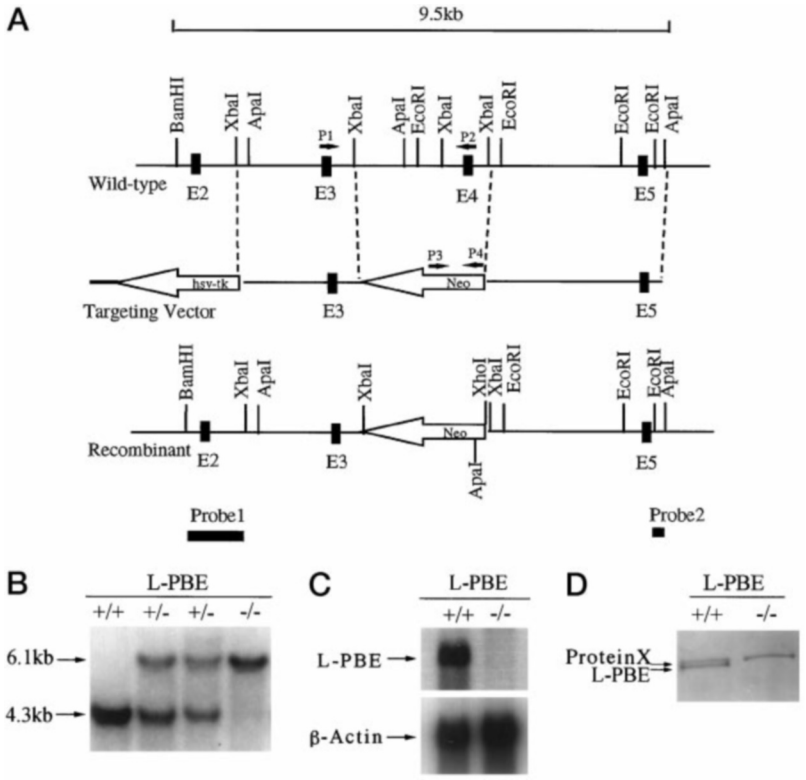

FIG. 1. **Generation of L-PBE-deficient mice.** *A*, schematic representation of the mouse L-PBE gene, targeting vector, and structure of the locus following gene targeting. Exons 2–5 (*E2* to *E5*) in the L-PBE gene are shown as *closed boxes*. Restriction sites are indicated. Locations of hybridization probes (probes 1 and 2) used for Southern blot analysis and of primers (*P1* to *P4*) used for polymerase chain reaction are shown. *B,* Southern blot analysis of genomic DNA. Genomic DNA (5 μg) isolated from tail tips of pups was digested with *Bam*HI and *Eco*RI and hybridized with the 5′-probe (probe 1 shown in *A*). *Lanes*: L-PBE$^{+/+}$ wild type, L-PBE$^{+/-}$ heterozygous, L-PBE$^{-/-}$ homozygous mice. *C,* Northern blot analysis using poly(A$^+$) RNA (5 μg/*lane*) isolated from liver probed with L-PBE or β-actin cDNA. *D,* Western blot analysis of liver homogenates for L-PBE expression in wild type (+/+) and L-PBE null (−/−) mice. The antibodies recognize L-PBE (*lower band*) and also an unidentified protein x (*upper band*) in the wild type mice. In L-PBE null mice only the *upper band* is identifiable, but not the band representing L-PBE.

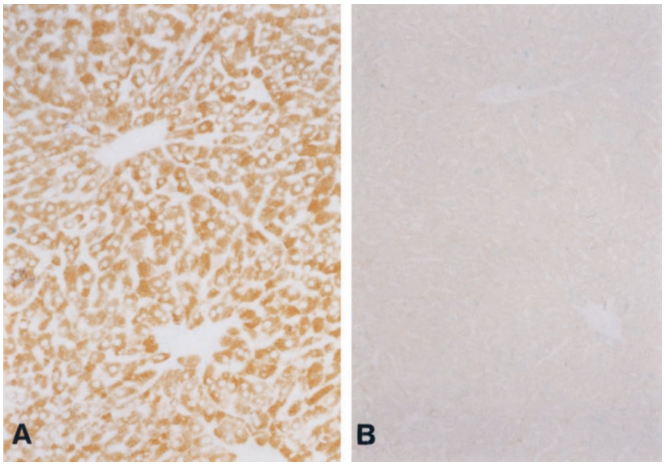

FIG. 2. **Immunoperoxidase staining for L-PBE in the liver.** Wild type mouse (*A*) and L-PBE$^{-/-}$ mice (*B*) were fed ciprofibrate (0.0125% in diet) for 2 weeks, and sections of liver were processed for immunohistochemical localization of L-PBE using antibodies against L-PBE. Intense cytoplasmic granular staining for L-PBE is seen in the liver of wild type mouse but not in L-PBE$^{-/-}$ mouse.

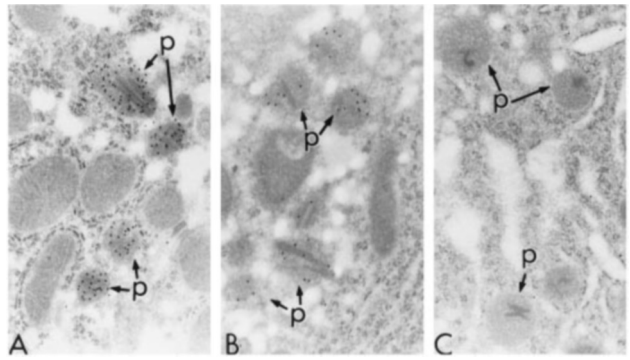

FIG. 3. **Immunogold localization of catalase and L-PBE in liver peroxisomes.** *A*, catalase localization in L-PBE$^{-/-}$ mouse liver. Note the presence of gold particles (*black dots*) over peroxisome (*p*) matrix representing catalase antigenic sites. *B* and *C* represent liver sections from wild type mouse and L-PBE$^{-/-}$ mouse, respectively, stained for L-PBE. No gold particles are seen over peroxisomes (*p*) in L-PBE$^{-/-}$ mouse liver.

randomly distributed in the cytoplasm, and appear as diaminobenzidine-positive brown granules (Fig. 4*E*). The numerical density of these organelles in L-PBE$^{-/-}$ mice on normal diet appeared similar to that observed in wild type mice (Fig. 4*F*). Thus, disruption of L-PBE gene fails to induce spontaneous peroxisome proliferation such as that encountered in liver cells of mice lacking AOX (Fig. 4, *G* and *H*).

Analysis of Fatty Acid-metabolizing Enzymes—The constitutive and inducible levels of fatty acid-metabolizing enzymes in livers of L-PBE$^{-/-}$ and wild type mice were evaluated by immunoblotting. Constitutive levels of expression of several peroxisomal (AOX, PTL, D-PBE, carnitine octanoyltransferase, SCPx, urate oxidase, and CTL) and mitochondrial (VLCAD, LCAD, medium chain acyl-CoA dehydrogenase, and short chain acyl-CoA dehydrogenase) enzymes were similar in wild type and L-PBE$^{-/-}$ mice (Fig. 5). The hepatic levels of AOX, PTL, D-PBE, carnitine octanoyltransferase, LCAD, and medium chain acyl-CoA dehydrogenase were increased in wild type and L-PBE$^{-/-}$ mice fed ciprofibrate for 2 weeks (Fig. 5). In wild type mice treated with ciprofibrate, hepatic levels of L-PBE protein increased substantially, and as expected, this protein was not detected in L-PBE$^{-/-}$mice maintained on control or ciprofibrate-containing diet (Fig. 5). These livers showed the presence of a nonspecific, cross-reacting band described in Fig. 1*D*, and this protein was not induced in L-PBE$^{-/-}$ mice treated with a peroxisome proliferator. Ciprofibrate did not increase the levels of SCPx, CTL, VLCAD, and short chain acyl-CoA dehydrogenase in wild type and L-PBE$^{-/-}$ mouse liver.

We also measured total hepatic β-oxidation using palmitic acid in mice fed either a control or ciprofibrate-containing diet. The basal level of total fatty acid β-oxidation was similar in wild type and L-PBE$^{-/-}$ mice. As expected, a 4- to 6-fold in-

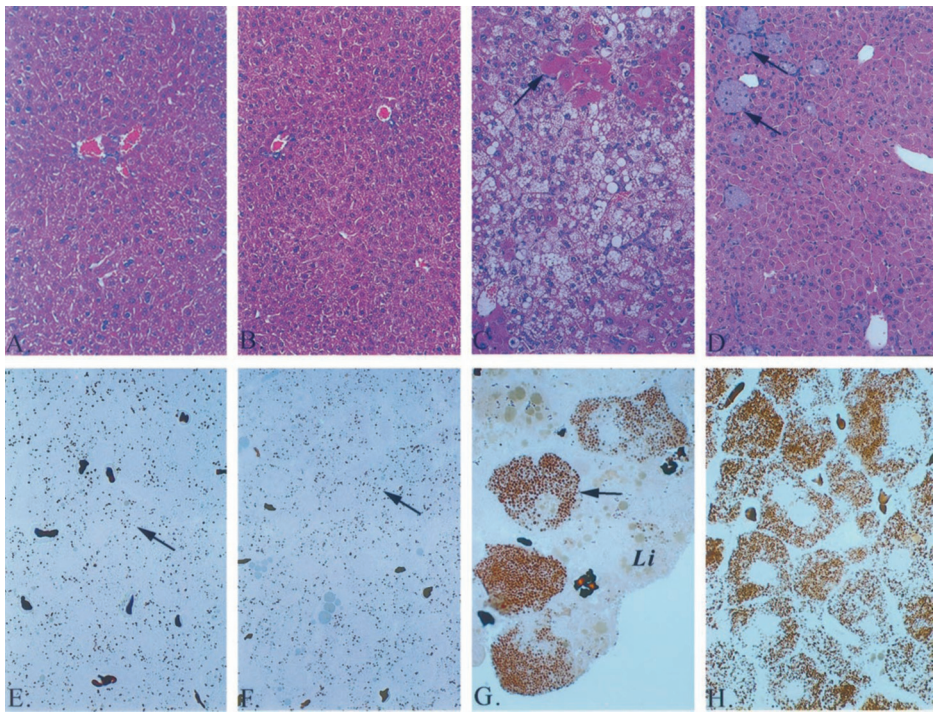

FIG. 4. **Liver morphology and changes in peroxisome population in L-PBE$^{-/-}$ and AOX$^{-/-}$ mice.** *A-D,* liver sections stained with hematoxylin and eosin. *A*, L-PBE$^{-/-}$ mouse. *B*, wild type litter mate. *C*, young AOX$^{-/-}$ mouse with microvesicular fatty change and few regenerated hepatocytes (*arrows*) with abundant eosinophilic cytoplasm, reflective of spontaneous peroxisome proliferation (see *G* below). *D,* older AOX$^{-/-}$ mouse liver with regenerated hepatocytes containing granular eosinophilic cytoplasm and scattered foamy lipid-laden macrophages (*arrows*). *E–H*, sections of liver that were processed for the cytochemical localization of peroxisomal catalase (11). L-PBE null mouse liver (*E*) and wild type mouse liver *(F)* show few peroxisomes in hepatocytes (*brown dots*, *arrows*). *G*, liver of a young AOX$^{-/-}$ mouse with numerous peroxisomes (*arrows*) in few liver cells such as those depicted by *arrows* in *C* above, whereas hepatocytes with microvesicular fatty change (*Li*) show few or no detectable peroxisomes. *H*, in older AOX−/− mice, all regenerated liver cells (*see D above*) show extensive spontaneous peroxisome proliferation.

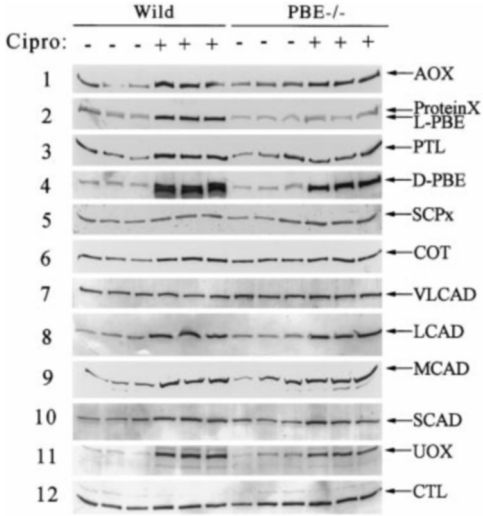

FIG. 5. **Immunoblot analysis of selected fatty acid-metabolizing and other enzymes in liver.** Liver homogenates from L-PBE$^{-/-}$ and L-PBE$^{+/+}$ mice fed either control or ciprofibrate (*Cipro*)-containing diet were subjected to SDS-polyacrylamide gel electrophoresis and immunoblotting (3 mice each group). AOX (5 μg), L-PBE (10 μg; note only the upper band, representing protein x, is present in L-PBE$^{-/-}$ mouse liver), PTL (10 μg); D-PBE (20 μg); SCPx (10 μg); carnitine octanoyltransferase (*COT*) (l0 μg); VLCAD (20 μg), LCAD (20 μg), medium chain acyl-CoA dehydrogenase (*MCAD*) (20 μg); short chain acyl-CoA dehydrogenase (*SCAD*) (10 μg); urate oxidase (*UOX*) (2 μg), and CTL (2 μg).

crease in total hepatic β-oxidation activity occurred in wild type mice treated with ciprofibrate, and the response of L-PBE$^{-/-}$ mice was essentially similar (data not presented). In contrast, the ciprofibrate-induced increase in the activity of cyanide-insensitive (peroxisomal) fatty acid β-oxidation system in L-PBE$^{-/-}$ mouse liver was ~75% that observed in wild type mice treated with ciprofibrate (data not presented).

Induction of mRNAs—Constitutive levels of acyl-CoA synthetase, AOX, PTL, CYP4A1, CYP4A3, D-PBE, and fatty acid-binding protein mRNAs were similar in the livers of both wild type and L-PBE$^{-/-}$ mice, indicating that unlike in AOX$^{-/-}$mice, there is no spontaneous up-regulation of PPARα-regulated genes in L-PBE$^{-/-}$ mice (Fig. 6). Following treatment with ciprofibrate, a 10-to 20-fold increase in liver AOX, PTL, CYP4A1, and CYP4A3 mRNA levels occurred in both wild type and L-PBE null mice, and the PTL, CYP4A1, and CYP4A3 increases were similar to spontaneous increases occurring in AOX$^{-/-}$mice (Fig. 6). Fig. 6 also confirms the expected absence of AOX and L-PBE mRNAs in the livers of AOX$^{-/-}$ and of L-PBE$^{-/-}$ mice, respectively. The spontaneous increase in L-PBE mRNA in AOX$^{-/-}$ mouse liver is comparable in magnitude to that occurring in ciprofibrate-treated wild type mouse (Fig. 6). We also found ~5-fold increase in D-PBE mRNA level in the liver of both wild type and L-PBE$^{-/-}$ mice treated with ciprofibrate.

Blunted Peroxisome Proliferative Response in L-PBE$^{-/-}$ Mouse Liver—Rats and mice treated with peroxisome proliferators such as ciprofibrate and Wy-14,643 exhibit abundant peroxisome proliferation in hepatocytes with peroxisomes occupying ~20 to 25% of cytoplasmic volume (6, 8). In AOX$^{-/-}$ mice we also found profound spontaneous proliferation of peroxisome, and such changes have been ascribed to sustained activation of PPARα by endogenous ligands that require AOX for metabolism or inactivation (10). We first established that deficiency of L-PBE neither caused spontaneous peroxisome proliferation nor led to an increase in protein and mRNA levels of genes regulated by PPARα. We then evaluated the impact of L-PBE gene disruption on peroxisome proliferation induced by peroxisome proliferators (Fig. 7). Light microscopic analysis of liver sections processed for cytochemical localization of catalase revealed massive proliferation of peroxisomes in liver cells of wild type mice treated with either ciprofibrate or Wy-14,643 for 2 weeks (Fig. 7*A*). In contrast, peroxisome-proliferative response appeared blunted in L-PBE$^{-/-}$ mouse liver (Fig. 7*B*). These observations were confirmed at the ultrastructural level in that peroxisome proliferation appeared robust in peroxisome proliferator-treated wild type mice but subdued in L-PBE$^{-/-}$ mouse liver cells (not illustrated). In L-PBE$^{-/-}$ mice treated with peroxisome proliferators, peroxisomal profiles tended to be smaller than those seen in wild type liver. Analysis of liver samples by SDS-polyacrylamide gel electrophoresis showed no

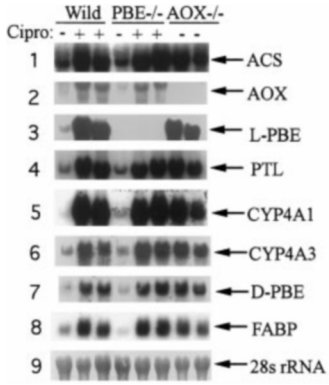

FIG. 6. **Northern blot analysis of total RNA extracted from liver.** Total RNA (20 μg) from L-PBE$^{-/-}$ and wild type littermate mice on control (−) or ciprofibrate (*Cipro*, 0.0125% w/w)-containing diet (+) for 2 weeks was hybridized with ^{32}P-labeled cDNA probes as indicated. Liver RNA from 6-month-old AOX null mice on control diet is used for comparison to show spontaneous up-regulation of PPARα-controlled genes in AOX$^{-/-}$ mouse liver. Acyl-CoA synthetase (*ACS*), AOX, L-PBE, PTL, CYP4A1, CYP4A3, D-PBE, and fatty acid-binding protein (*FABP*) genes are transcriptionally activated by PPARα. D-PBE mRNA is also increased but to a lesser extent than that of L-PBE in wild type mice fed ciprofibrate. 28 S RNA is used as loading indicator.

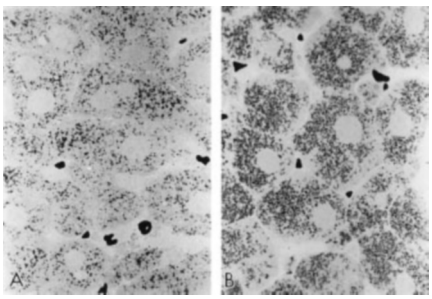

FIG. 7. **Response of PBE$^{-/-}$ and wild type littermate mice to a peroxisome proliferator.** Ciprofibrate, a peroxisome proliferator, was fed in the diet for 2 weeks (0.0125% w/w). Livers were processed for cytochemical localization of peroxisomal catalase. L-PBE $^{-/-}$ (*A*) and wild type mice (*B*) were treated with ciprofibrate. Peroxisomes appear as *black dots* in these *black and white* photographs; in L-PBE$^{-/-}$ mouse liver, ciprofibrate-induced peroxisome proliferation is somewhat subdued.

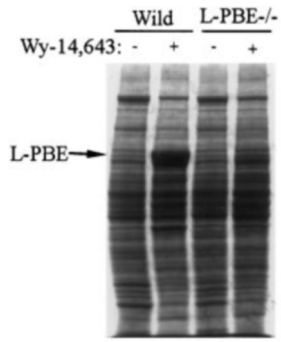

FIG. 8. **SDS-polyacrylamide gel electrophoresis of liver homogenates.** Liver samples from wild type and L-PBE$^{-/-}$ mice fed control diet (−) or a diet containing Wy-14,643 (+) were subjected to SDS-polyacrylamide gel electrophoresis, and the gel was stained with Coomassie Brilliant R Blue. Note the presence of massive amounts of 78-kDa L-PBE protein in the liver of wild type mouse treated with Wy-14,643 (*arrow*); it is not present in L-PBE$^{-/-}$mice.

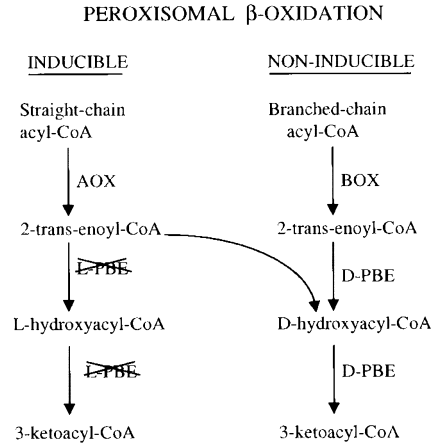

FIG. 9. **Schematic representation of peroxisome proliferator inducible, L-hydroxy-specific, classical peroxisomal β-oxidation system and the noninducible D-hydroxy-specific system.** In mice deficient in L-PBE, the straight chain enoyl-CoAs are most likely diverted to the noninducible branched chain β-oxidation pathway for metabolism by D-PBE. In contrast, in AOX$^{-/-}$ mice, the straight chain fatty acyl-CoAs and possibly other PPARα ligands are not metabolized because of the absence of AOX, and these substrates are not diverted to a noninducible system for degradation by branched chain acyl-CoA oxidase, thus causing sustained activation of PPARα.

increase in the 78-kilodalton L-PBE protein in L-PBE−/− mice treated with a peroxisome proliferator (Fig. 8).

Liver Cell Proliferation—Increased liver cell proliferation has been noted in mice deficient in AOX $^{-/-}$, attributable in part to cell loss resulting from extensive steatosis (10). Because peroxisome proliferators are also known to induce transient liver cell proliferation (8), we assessed the impact of L-PBE gene disruption on hepatocyte proliferation induced by the administration of a peroxisome proliferator in the diet for 3 days. No significant difference in hepatocyte nuclear labeling was found between wild type and L-PBE$^{-/-}$ mice treated with a peroxisome proliferator (data not shown).

DISCUSSION

The classical peroxisome proliferator-inducible L-hydroxy-specific peroxisomal β-oxidation system that acts on long and very long straight chain acyl-CoAs, long chain dicarboxylyl-CoAs, and the CoA esters of prostaglandins consists of AOX, L-PBE, and PTL (2, 3). The second noninducible D-3-hydroxy-specific peroxisomal β-oxidation system that acts on branch chain acyl-CoAs also contains three enzymes namely, branched chain acyl-CoA oxidase, D-PBE, and SCPx (3, 4, 15). Straight chain acyl-CoAs are almost exclusively metabolized by classical AOX and not by D-hydroxy-specific branched chain acyl-CoA oxidase, although the enzymes of D-hydroxy-specific β-oxidation pathway reveal minor catalytic activity toward straight chain acyl-CoAs (3, 4, 15). This assumption is supported by the observations in mice deficient in classical AOX as they exhibit sustained up-regulation of PPARα-induced genes along with spontaneous peroxisome proliferation in liver parenchymal cells, indicating that this L-hydroxy-specific AOX is crucial for metabolically degrading biological ligands of PPARα (10, 16). Because this classical β-oxidation system degrades long and very long straight chain fatty acids, long chain dicarboxylic acids, and prostaglandins or their respective CoAs, it is reasonable to conclude that these and possibly other yet to be identified substrates of L-hydroxy-specific AOX act as natural ligands of PPARα (10). These AOX-deficient mice also highlight the fact that substrates of this classical AOX that function as PPARα ligands are not degraded by D-hydroxy-specific branched chain acyl-CoA oxidase. Here we have described the generation and initial characterization of a mouse homozygous for a targeted disruption of L-PBE, the enzyme immediately distal to AOX in the classical L-hydroxy-specific β-oxidation pathway. L-PBE$^{-/-}$mice, in combination with AOX$^{-/-}$ (10), PPAR$\alpha^{-/-}$ (17), X-ALD$^{-/-}$ (X-linked adrenoleukodystrophy

gene (18)), SCPx $^{-/-}$ (19), LCAD$^{-/-}$ (20) and other mouse models should prove valuable in exploring the functional role and/or redundancy of metabolic pathways in lipid metabolism. These mutant mice will also be valuable in investigating the role of the enzymes of lipid metabolism in regulating the function of PPARα and possibly other receptors (10, 20).

There are several lines of evidence that support the view that the mice we generated in this study contain a null mutation in the L-PBE gene. The gene targeting construct we used was designed to eliminate the entire exon 4, and the selectable gene cassette used to disrupt the L-PBE gene introduced nonsense mutation in all reading frames. Polymerase chain reaction as well as Southern blot analysis revealed that ES cells contained the correct targeted event, and Northern blot analysis revealed that liver from L-PBE$^{-/-}$ mice fed either a control diet or peroxisome proliferator-containing diet did not contain a detectable message corresponding to the L-PBE probe. The L-PBE$^{-/-}$ mice displayed no authentic L-PBE protein on Western blot analysis; the L-PBE antibody we used was raised against rat L-PBE, and in mouse liver, it recognized a nonspecific protein band, designated protein x, the identity of which, however, remains to be determined (Fig. 1*D*). By immunogold technique, this protein x was detected in mitochondria and not in peroxisomes of L-PBE$^{-/-}$mice, further confirming the L-PBE null mutation. It is also worth noting that this protein x was not induced in the livers of wild type and L-PBE$^{-/-}$ mice treated with peroxisome proliferators. Peroxisome of L-PBE$-/-$ mice did not reveal any staining for L-PBE by immunogold procedure (Fig. 3*C*), and when these animals were treated with a peroxisome proliferator, the liver parenchymal cells failed to show any immunohistochemically detectable L-PBE protein (Fig. 2). These observations unequivocally establish the disruption of L-PBE gene, and the absence of L-PBE mRNA and protein, therefore, establish the functional inactivation of this gene.

The striking results observed in these L-PBE$^{-/-}$ mice were the absence of hepatic steatosis and of spontaneous peroxisome proliferation such as that found in the livers of young AOX$^{-/-}$ mice (10). These observations provide strong evidence that the classical AOX of the L-hydroxy-specific β-oxidation system is responsible for the metabolism of all putative ligands of PPARα and that L-PBE enzyme immediately downstream of AOX is not essential for the successful completion of the L-hydroxy-specific β-oxidation. It would appear that once the long and very long straight chain acyl-CoAs, long chain dicarboxylyl-CoAs, and the CoA esters of prostaglandins are converted into their respective enoyl-CoAs by the classical AOX, these can be metabolized by D-PBE of the D-hydroxy-specific peroxisomal β-oxidation system (Fig. 9) or even by the mitochondrial β-oxidations system. In essence, the AOX null and L-PBE null mouse models we generated convincingly prove that classical AOX is pivotal for the metabolic degradation of PPARα ligands and not the branched chain acyl-CoA oxidase of the second system. Further studies, however, are needed to rule out the possibility that straight chain enoyl-CoAs generated by classical AOX, if left unmetabolized, serve as PPARα ligands (10, 21). This issue can be explored by generating mice deficient in both L-PBE and D-PBE and characterizing their liver phenotype.

Of further interest is that L-PBE$^{-/-}$ mice, when challenged with a peroxisome proliferator, exhibited somewhat blunted hepatic peroxisome proliferative response, although there were no significant differences in other immediate or early pleiotropic responses attributable to PPARα activation, with the single notable, but expected exception that L-PBE mRNA and protein are undetectable in L-PBE$^{-/-}$ mouse livers. Thus, the blunting of peroxisome proliferative response is attributed to the absence of L-PBE protein in L-PBE null animals. It is important to note that L-PBE, a 78-kilodalton protein, is massively induced in the livers of wild type mice exposed to peroxisome proliferators (22). This protein, once called peroxisome proliferator-activated polypeptide (22), becomes the most abundant protein in the livers of peroxisome proliferator-treated rats and mice, contributing substantially to the morphological phenomenon of peroxisome proliferation. The L-PBE null mutation abolishes the inducibility of L-PBE in response to peroxisome proliferators, and this most likely accounts for the blunting of peroxisome proliferative response, because all other PPARα responsive genes in L-PBE$^{-/-}$mice are up-regulated. Therefore, it is conceivable that changes in the levels of expression of L-PBE gene in nonrodent species in response to peroxisome proliferators may influence the morphological phenomenon of peroxisome proliferation, whereas other effects of these PPARα ligands in nonrodent species may be similar to those seen in rats and mice. It would be of great interest to investigate whether L-PBE$^{-/-}$mice develop liver tumors following chronic exposure to peroxisome proliferators, despite the subdued nature of peroxisome proliferative response, because all other PPARα-regulated genes are up-regulated.

REFERENCES

1. Lazarow, P. B., and de Duve, C. (1976) *Proc. Natl. Acad. Sci. U. S. A.* **73,** 2043–2046
2. Reddy, J. K., and Mannaerts, G. P. (1994) *Annu. Rev. Nutr.* **14,** 343–370
3. Hashimoto, T. (1999) *Neurochem. Res.*, in press
4. Baumgart, E., Vanhooren, J. C. T., Fransen, M., Marynen, P., Puype, M., Vanderkerckhove, J., Leunissen, J. A. M., Fahimi, H. D., Mannaerts, G. P., and Van Veldhoven, P. P. (1996) *Proc. Natl. Acad. Sci. U. S. A.* **93,** 13748–13753
5. Mori, T., Tsukumoto, T., Mori, H., Tashiro, Y., and Fujiki, Y. (1991) *Proc. Natl. Acad. Sci U. S. A.* **88,** 4338–4342
6. Reddy, J. K., and Krishnakantha, T. P. (1975) *Science* **190,** 787–789
7. Issemann, I., and Green, S. (1990) *Nature* **347,** 645–650
8. Rao, M. S., and Reddy, J. K. (1987) *Carcinogenesis* **8,** 631–636
9. Gonzalez, F. J. Peters, J. M., and Cattley, R. C. (1998) *J. Natl. Cancer Inst.* **90,** 1702–1709
10. Fan, C-Y., Pan, J., Usuda, N., Yeldandi, A. V., Rao, M. S., and Reddy, J. K. (1998) *J. Biol. Chem.* **273,** 15639–15645
11. Ishii, N., Hijikata, M., Osumi, T., and Hashimoto, T. (1987) *J. Biol. Chem.* **262,** 8144–8150
12. Ausubel, F. M., Brent, R., Kingston, R. E., Moore, D. D., Seidman, J. G., Smith, J. A., and Struhl, K. (eds) (1993) *Current Protocols in Molecular Biology*, John Wiley & Sons, Inc., New York
13. Usuda, T., Nakazawa, A., Terasawa, M., Reddy, J. K., and Nagata, T. (1996) *Ann. N. Y. Acad. Sci.* **804,** 297–309
14. Aoyama, T., Peters, J. M., Iritani, N., Nakajima, T., Furihata, K., Hashimoto, T., and Gonzalez, F. J. (1998) *J. Biol. Chem.* **273,** 5678–5684
15. Jiang, L. L., Kurosawa, T., Sato, M., Suzuki, Y., and Hashimoto, T. (1997) *J. Biochem.* (*Tokyo*) **121,** 506–513
16. Forman, B. M., Chen, J., and Evans, R. M. (1997) *Proc. Natl. Acad. Sci. U. S. A.* **89,** 4653–4657
17. Lee, S. S-T., Pineau, T., Drago, J., Lee, E. J., Owens, J. W., Kroetz, D. L., Fernandez-Salguero, P. M., Westphal, H., and Gonzalez, F. J. (1995) *Mol. Cell. Biol.* **15,** 3012–3022
18. Lu, J-F., Lawler, A. M., Watkins, P. A., Powers, J. M., Moser, A. B., Moser, H. W., and Smith, K. D. (1997) *Proc. Natl. Acad. Sci. U. S. A.* **94,** 9366–9371
19. Seedorf, U., Raabe, M., Ellinghaus, P., Kannenberg, F., Fobker, M., Engel, T., Denis, S., Wouters, F., Wirtz, K. W. A., Wanders, R. J. A. Maeda, N., and Assmann, G. (1998) *Genes Dev.* **12,** 1189–1201
20. Kurtz, D. M., Rinaldo, P., Rhead, W. J., Tian, L., Millington, D. S., Vockley, J., Hamm, D. A., Brix, A. E., Lindsey, J. R., Pinkert, C. A., O'Brien, W. E., and Wood, P. A. (1998) *Proc. Natl. Acad. Sci. U. S. A.* **95,** 15592–15597
21. Faergeman, N. J., and Knudsen, J. (1997) *Biochem. J.* **323,** 1–12
22. Reddy, J. K., and Kumar, N. S. (1977) *Biochem. Biophys. Res. Commun.* **77,** 824–829